



Enhancing Power System Resilience: Load Shedding and Equilibrium Optimization in FACTS Devices Allocation

Mehdi Shafiee^{1*}

¹Department of Electrical Engineering, Technical and Vocational University (TVU), Tehran, Iran

ARTICLE INFO

Article Type:
Original Research

Received: 01.20.2025
Revised: 02.07.2025
Accepted: 04.19.2025

Keyword:
FACTS Devices
System security
Load shedding
EOA
UPFC
SVC

***Corresponding Author:**
Mehdi Shafiee
Email: m-shafiee@tvu.ac.ir

ABSTRACT

The efficient management of power systems is becoming increasingly crucial as the demand for electricity rises and renewable energy sources are integrated. Ensuring system stability while managing costs presents a significant challenge for grid operators and planners. This study investigates the viability of using an equilibrium optimization algorithm (EOA) technique to determine the most effective distribution of multi-type Flexible AC Transmission System (FACTS) devices in order to maximize system security and reduce the annual investment expenditure on FACTS devices. In this process, voltage limits for buses and FACTS devices are considered as constraints, and two types of FACTS devices—Static VAR Compensator (SVC) and Unified Power Flow Controller (UPFC)—are analyzed: two cases, consisting of single-type devices (the same kind of FACTS devices) and multi-type devices (a combination of SVC and UPFC) are considered. In order to assign FACTS devices, simulations are performed on IEEE 30 bus test system using a load shedding technique to optimize costs. The simulations' outcomes are encouraging and may be useful for electrical restructuring.



Introduction

One The complexity of a power system, comprising of various generators, transmission lines, different types of loads and transformers, can be compounded by faults or increasing power demand. This state is known as a contingency state, and the operations needed to rectify it are referred to as contingency control or corrective control. If corrective control is not considered in the power system design, it can lead to an increased risk of voltage collapse and system instability. Consequently, there has been a growing interest in the utilization of FACTS devices as a corrective action control [1; 2]. Additional roles of corrective control include distributed generation [3-5], corrective switching in transmission systems [6], and load shedding [7; 8].

In order to meet voltage limits in both standard and emergency scenarios, reactive power planning requires the best possible allocation and the identification of new reactive power sources in terms of size and type [9]. Research and findings have demonstrated the aptitude of FACTS devices for steady-state and transient power system analysis [10]. Specific papers have concentrated on discovering appropriate positions for FACTS devices to enhance power system security and loadability [11; 12]. The optimal distribution of these devices in deregulated power systems has been documented in [13; 14]. Heuristic methodologies and intelligent algorithms have been employed in some research papers to determine the optimal placement of FACTS devices for corrective action control [15; 16]. In this study, an EOA [17] that amalgamates Particle Swarm Optimization (PSO) and genetic algorithms (GA) evolutionary operators is employed to achieve the optimal placement of multi-type FACTS devices in order to minimize the annual expenditure of such apparatuses. Two distinct devices with distinct characteristics are chosen and modelled for steady-state analysis. The goal of minimizing load shedding costs is achieved through the implementation of the EOA algorithm and corrective control action. Steady-state simulations are executed on the IEEE 30-bus test system to assess the efficacy of the proposed algorithm, providing positive results.

FACTS devices Modelling and Control

The Electrical Power Research Institute (EPRI) introduced FACTS technology in the 1980s. This technology involves the use of power electronics, ranging from tens to hundreds of megawatts, to convert and switch electrical power. FACTS devices use devices like MOSFETs, IGBTs, GTOs, and other appropriate power electronic devices as controlled switches [18]. This paper evaluates two different FACTS devices - SVC and UPFC - for their potential to improve the security of a power system by placing them in a suitable location.

SVC

The SVC system is constructed of capacitors, thyristors, and inductances. The components of this device are illustrated in Figure 1. SVCs could be model by two methods. The first approach conceptualizes SVC as an adjustable impedance that automatically adjusts to maintain voltage control. This is referred to as the passive model, however its major drawback is that the nodal admittance matrix constantly fluctuates when the power grid operates under varying conditions [19].

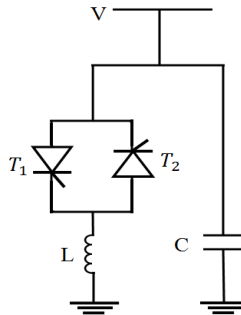


Figure 1. Series Schematic diagram of SVC

The second model, referred to as the active model, conceptualizes SVC as a node-injected power source. This model utilizes active sources in its equivalent circuit, which can conveniently be integrated into Power flow (PF), Optimal Power flow (OPF) and Voltage Stability studies [20]. Generally speaking, the active model employs the reactive power injected or consumed by the SVC as its state variable (Q_s). The operational technical limits of this variable are:

$$\begin{aligned}
 Q_{\min} &\leq Q_s \leq Q_{\max} \\
 Q_{\max} &= B_{ind} V_{ref}^2 \\
 Q_{\min} &= B_{cap} V_{ref}^2
 \end{aligned} \tag{1}$$

Where B_{ind} and B_{cap} are capacitive susceptance and inductive susceptance and V_{ref} is the reference for the bus voltage [21].

UPFC

The UPFC is composed of two Voltage Source Converters (VSCs) which are connected to a shared capacitor on the Direct Current (DC) side, along with a unified control system. The schematic representation and corresponding electrical model of the UPFC are illustrated in Figure 2. the UPFC has the capability to control active power flow, reactive power flow and voltage magnitude at the UPFC terminals independently or simultaneously. Alternatively, it can be set to control none of them [22].

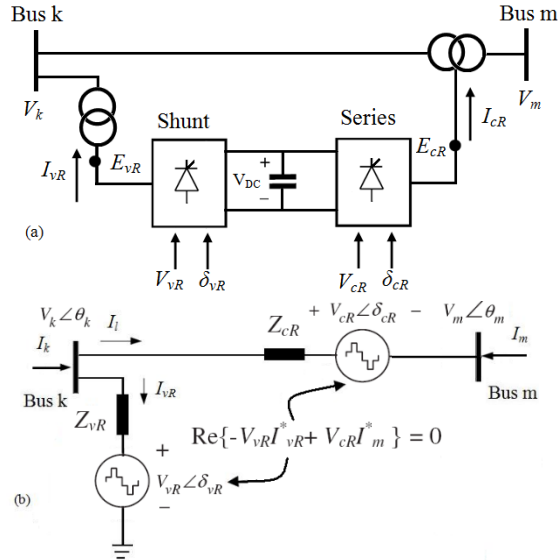


Figure 2. a) Basic UPFC model, b) electrical model of UPFC

The shunt converter sources the active power required by the series converter from the AC network and sends it to bus m over the DC link. An elevated nodal voltage at bus m is the result of superimposing the series converter's output voltage on the nodal voltage at bus k. While the δ_{cR} phase angle dictates how power flow will be controlled, the size of the V_{cR} output voltage regulates voltage [23].

The shunt converter may contribute to the active power exchange between the series converter and the AC system, and can also independently regulate voltage magnitude at the point of connection with the AC system by generating or absorbing reactive power.

A parallel-connected voltage source, a series-connected voltage source, and an active power restriction equation that connects the two voltage sources make up the UPFC equivalent circuit shown in Figure 2(b). Through their inductive reactance, the two voltage sources—which stand in for the voltage source converter (VSC) transformers—are connected to the alternating current (AC) system. Proper formulations for the constraint equation and the two voltage sources in a three-phase UPFC can be created as follows:

$$\begin{aligned}
 E_{vR}^\rho &= V_{vR}^\rho (\cos \delta_{vR}^\rho + j \sin \delta_{vR}^\rho) \\
 E_{cR}^\rho &= V_{cR}^\rho (\cos \delta_{cR}^\rho + j \sin \delta_{cR}^\rho) \\
 \text{Re}\{-V_{vR}^\rho I_{vR}^{*\rho} + V_{cR}^\rho I_m^{*\rho}\} &= 0
 \end{aligned} \tag{2}$$

Where ρ stands for phase values a, b, and c. V_{vR} and δ_{vR} stand for the voltage source's programmable magnitudes ($V_{vRmin} \leq V_{vR} \leq V_{vRmax}$) and phase angle ($0 \leq \delta_{vR} \leq 2\pi$) of the shunt converter. Magnitude V_{cR} and phase angle δ_{cR} of the voltage source representing the series converter are modified between limits ($0 \leq \delta_{cR} \leq 2\pi$) and $V_{cRmin} \leq V_{cR} \leq V_{cRmax}$, respectively.

The phase angle of the voltage injected into the series circuit determines the mechanism of power flow control. If the nodal voltage angle θ_k and δ_{cR} are in phase, the UPFC regulates the terminal voltage. When δ_{cR} is in quadrature with respect to θ_k , it acts as a phase shifter, controlling the flow of active power. When δ_{cR} is in quadrature with the line current angle, it acts as a variable series compensator, controlling the flow of active power. For all other values of δ_{cR} , the UPFC acts as a voltage regulator, variable series compensator, and phase shifter. As demonstrated in [23], the amplitude of the series-injected voltage determines how much power flow it can regulate.

The active model is preferred for modeling FACTS devices because it conceptualizes the SVC as a node-injected power source, making it more suitable for power flow and voltage stability studies. In contrast to the passive model, the active model does not require constant updates to the nodal admittance matrix, which enhances computational efficiency.

Proposed Algorithm

Equilibrium optimization algorithm

The EO algorithm is a new optimization algorithm that emanates from the dynamic equation of the mass balance. For a control volume, this dynamic equation characterizes the condensation of a non-reactive component as a function of diverse sink and source mechanisms [17]. Unlike traditional optimization techniques such as PSO and GA, the proposed EOA explicitly balances exploration and exploitation through its equilibrium pool and generation rate, leading to faster convergence and more reliable solutions for problems. The algorithm's main steps are as follows:

Step 1: Initialization

The parameter initialization and the particles initialization are the main stages of this step that are presented in the following:

- Determining the initial parameters of the EO algorithm:

These parameters are the population size, N_p , the maximum iterations' number, N_{iter}^{max} , the search space boundary conditions, and the exponential term parameters a_1 , a_2 , and G_p .

- Determining the initial particles of the EO algorithm:

Using Eq. 3, the initial particles of the EO algorithm are generated.

$$C_i^{initial} = C_{min} + r_i (C_{max} - C_{min}) \quad (3)$$

In this equation, $C_i^{initial}$ is the vector of particle i in the interval of $[C_{min} C_{max}]$ and r_i is a random number in $[0, 1]$.

Step 2: Fitness value evaluation for each particle

For the particles, a fitness value comparison between the current and previous iteration is done and the better fit will be saved.

Step 3: Create the pool of equilibrium.

The equilibrium pool and the particle concentration, C_{eq} , are created using Eqs. 4 and 5. This pool consists of the best-selected particle named $C_{eq(1)}$, $C_{eq(2)}$, $C_{eq(3)}$, and $C_{eq(4)}$. Also, their average is represented by $C_{eq(ave)}$. This step guarantees the ability for exploitation and exploration.

$$C_{eq} = \{C_{eq(1)}, C_{eq(2)}, C_{eq(3)}, C_{eq(4)}, C_{eq(ave)}\} \quad (4)$$

$$C_{eq(ave)} = (C_{eq(1)} + C_{eq(2)} + C_{eq(3)} + C_{eq(4)}) / 4 \quad (5)$$

Step 4: Exponential index and generation rate updating.

The EOA balances exploration and exploitation through its equilibrium pool, exponential index, and generation rate. The equilibrium pool ensures diversity, while the exponential index and generation rate dynamically adjust the search process to explore new regions and refine existing solutions. The exponential index is calculated using the following equations:

$$F = a_1 \text{sign}(r - 0.5)(e^{-\lambda t} - 1) \quad (6)$$

$$t = \left(1 - \frac{i_{iter}}{N_{iter}^{max}}\right)^{\left(a_2 \frac{i_{iter}}{N_{iter}^{max}}\right)} \quad (7)$$

In this equation, the exploration capability is controlled using the constant value, a_1 , and the exploitation capability is controlled using the constant value, a_2 . Also, i_{iter} and N_{iter}^{max} are the current iteration and the maximum iterations' number. The values of r and λ are random numbers in the interval $[0, 1]$.

The generation rate is calculated using the following equations:

$$G = G_0 e^{(-\lambda(t-t_0))} = G_0 F \quad (8)$$

$$G_0 = GCP(C_{eq} - \lambda C) \quad (9)$$

$$GCP = \begin{cases} 0.5r_1 & r_2 \geq GP \\ 0 & r_2 \leq GP \end{cases} \quad (10)$$

Where G and GCP are the generation rate and its control parameter, respectively. The generation probability is presented by GP . This parameter indicates the contribution of the generation probability for the procedure of updating. Also, r_1 and r_2 represent random numbers in the interval $[0, 1]$.

Step 5: Particle concentration updating.

The particle concentration is updated according to the following equation:

$$C_{new} = C_{eq} + (C - C_{eq})F + \frac{G}{\lambda V}(1 - F) \tag{11}$$

In this equation, the inward concentration of the control volume is denoted by C . The parameter V is assumed to be one.

Step 6: Until the Iter value reaches to N_{iter}^{max} , go to step 3.

Problem Formulation

Upon the occurrence of an emergency state due to a fault such as a load growth, it is imperative that the power system returns to its standard condition in the most expeditious manner. In order to accomplish this objective and improve system security, this paper aims to deploy FACTS devices while minimizing the annual corrective control costs. To this end, the annual cost of the FACTS devices is calculated and used as an objective function.

FACTS Devices Capital Expenditure

An examination of empirical evidence on reactive power supplies suggests that for lower power ratings, the cost of the device is augmented, whereas for higher power rates the cost is diminished. Figure 3 displays the expenditure costs of FACTS devices (e.g., SVC and UPFC) [24].

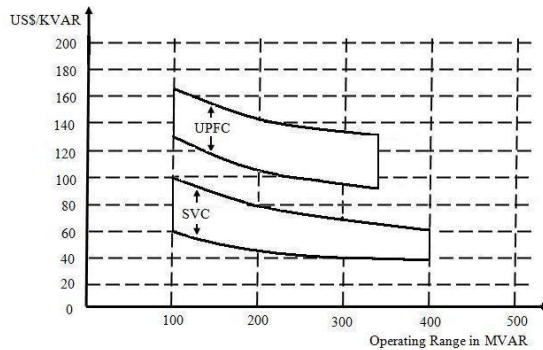


Figure 3. FACTS Devices Capital Expenditure

Depicted in Figure 3., in the problem formulation, it is supposed that the investment costs associated with FACTS devices can be a quadratic function:

$$\mu_i = a_2 Q_i^2 - a_1 Q_i + a_0 \tag{12}$$

The investment cost of FACTS devices, denoted by μ_i , and the sizes of the installed devices, denoted by Q_i , are expressed in terms of \$/KVAR and MVAR, respectively. The coefficients of Eq. 12 for SVC and UPFC can be found in the accompanying table which is generated by using a curve fitting technique to the data presented in Fig. 3 [25].

Optimization model

The initial investment cost as demonstrated by Equation 13 is presented in Equation 14 to be implemented in the problem.

$$F_{I0} = \sum_{i \in \theta} (\mu_i \cdot Q_i \cdot d_i) \quad (13)$$

Let θ be a set of potential locations for FACTS devices, and let Q_i be the size of the additional FACTS devices in site i (bus i for SVC and line i for UPFC). If site i is chosen for the expansion FACTS devices, $d_i=1$; if not, $d_i=0$. The following formula can be used to get the yearly investment costs (F_{It}):

$$F_{It} = \frac{i_r(1+i_r)^{D_y}}{(1+i_r)^{D_y} - 1} F_{I0} \quad (14)$$

Let i_r and D_y represent the FACTS devices' interest rate and lifespan, respectively. Therefore, it is possible to formulate the allocation of FACTS devices problem with the goal of minimizing annual investment costs while accounting for the power system's operating limitations:

$$\text{Minimize } F_{total} = F_{It} \quad (15)$$

$$\text{Subject to: } V_{\min,i} \leq V_i \leq V_{\max,i}$$

The highest and lowest permitted voltages in bus i are $V_{\max,i}$ and $V_{\min,i}$, respectively. Furthermore, as further constraints, the power flow equations ought to be incorporated into the formulation:

$$g(V, \theta) = 0 \quad (16)$$

where:

$$g(V, \theta) = \begin{cases} P_m(V, \theta) - P_m^{net} \\ Q_m(V, \theta) - Q_m^{net} \\ P_n(V, \theta) - P_n^{net} \end{cases} \quad (17)$$

The parameters P_m , Q_m Calculated active and reactive power for PQ bus m , P_m^{net} , Q_m^{net} Specified active and reactive power for PQ bus m , P_n , P_n^{net} Calculated and specified active power for PV bus n , V Voltage magnitude at different buses, θ Voltage phase angle at different buses.

The constraints associated with FACTS devices consist of:

$$\begin{aligned} -0.8X_L &\leq X_{UPFC} \leq 0.2X_L \\ 100MVAR &\leq Q_{UPFC} \leq 320MVAR \\ 100MVAR &\leq Q_{SVC} \leq 400MVAR \end{aligned} \quad (18)$$

Where, X_{UPFC} , Reactance added to the line by placing UPFC, X_L Reactance of the line where UPFC is located, Q_{UPFC} and Q_{SVC} Reactive power injected by placing UPFC and SVC.

Sensitivity analysis for Sites Selection of FACTS Devices

The essential sage in the process of allocating FACTS devices is the selection of candidate sites for the placement of new reactive power devices. While it would be ideal to install unlimited FACTS devices at all buses, it is not economically feasible and so a limited number of candidate buses must be chosen.

To ascertain which potential sites are suitable for the installation of SVC and UPFC voltage control FACTS devices, participation parameters obtained from sensitivity analysis are applied as voltage indexes. These parameters are obtained by means of a Jacobian matrix:

$$\begin{bmatrix} \delta \\ V \end{bmatrix} = \begin{bmatrix} J_{11} & J_{12} \\ J_{21} & J_{22} \end{bmatrix}^{-1} \cdot \begin{bmatrix} P \\ Q \end{bmatrix} \quad (19)$$

When disregarding the influence of active power on the size of bus voltage, the voltage of every bus will be equivalent to equation (20):

$$V_i = \alpha_{i1} \cdot Q_1 + \dots + \alpha_{in} \cdot Q_n \quad (20)$$

Where α 's are participation factors. These values are normalized, with higher factors indicating buses that are more sensitive to voltage changes and thus prioritized for FACTS placement.

In conclusion, a load flow is conducted and the number of buses with the lowest voltage is selected in order to identify potential locations following an increase in the power system's load. Equation 20 is then produced by applying sensitivity analysis. It should be remembered that the buses with higher participation factors in equation 20 are the prospective sites.

Corrective control action using the EOA algorithm

The proposed design methodology for load-shedding and FACTS allocation algorithms based on the EOA process will be described in this section. As previously mentioned, the fitness function for the placement of FACTS devices is represented by the following equation:

$$J^c = F_{it} + J_1 + J_2 \quad (21)$$

The cost functions associated to the violations of the minimum and maximum voltage constraints are represented by J_1 and J_2 in this equation, which is written as follows:

$$\begin{aligned} J_1 &= pf_1 * abs(sign(V_{\min} - 0.95) - 1) \\ J_2 &= pf_2 * abs(sign(V_{\max} - 1.05) + 1) \end{aligned} \quad (22)$$

Penalty factors pf_1 and pf_2 are taken into account when determining whether the requirements in these equations are satisfied; if they are not, the fitness function rises, which may lead to the eradication of bacteria during regeneration.

In order to evaluate and compare the overall cost reductions, optimal load shedding is also used to establish corrective action control. The implementation of the EOA algorithm minimizes the expenses associated with load shedding while guaranteeing that the load power factor remains constant. Therefore, the following is the expression for the fitness function that is used for optimal load shedding:

$$J^{sh} = F_{L.Sh} + J_1 + J_2 \quad (23)$$

The parameters J_1 and J_2 are defined based on Eq. 22.

Ultimately, the cost savings attributed to the implementation of FACTS devices is determined using the following formula:

$$F_{saving} = F_{L.Sh} - F_{It} \quad (24)$$

The overall flowchart of the proposed technique is depicted in Figure 4 for illustrative purposes.

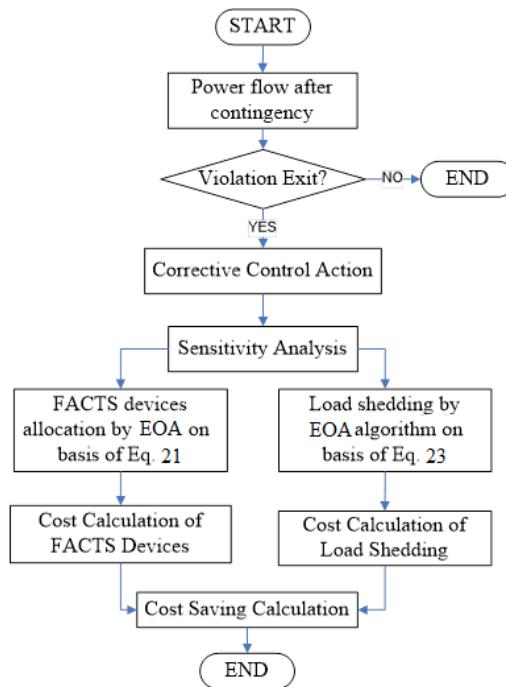


Figure 4. Overall Flowchart of the Proposed Technique

Results and Discussion

The effectiveness and efficiency of the suggested technique are evaluated in this work using an IEEE 30-bus test system, as shown in Figure 5 [26]. The interest rate (i_r) is 0.04 and the expected life period of FACTS devices (D_y) is 10 years [27].

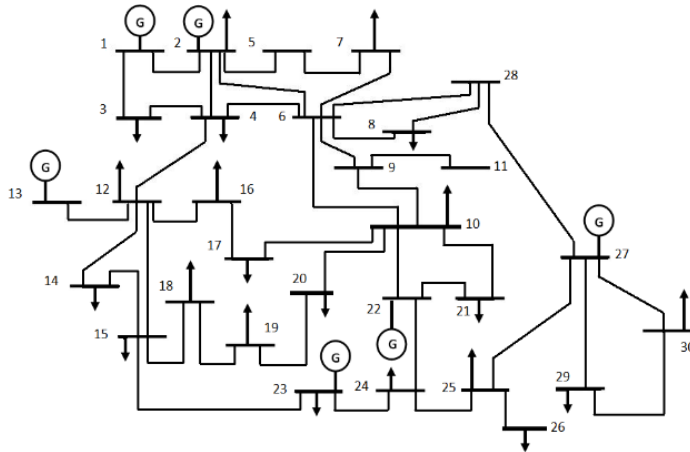


Figure 5. Diagram of IEEE 30-bus system

The voltage profile in the system's normal state, where all voltages remain within their permitted ranges, is shown in Figure 6. ($0.95 \text{ p.u.} < V < 1.05 \text{ p.u.}$).

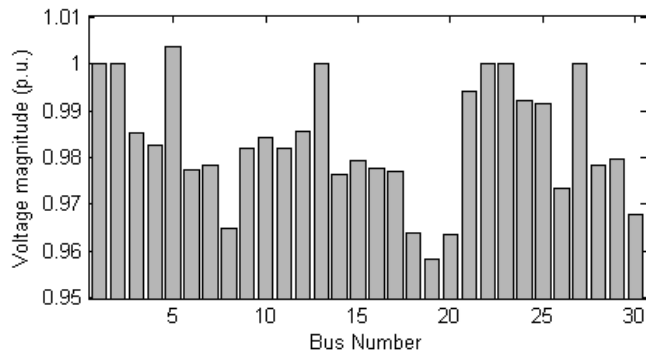


Figure 6. System Voltage profile in normal state

Considering the prevalence of overloading in power systems, a system analysis is performed at a high load level, assuming a 70% increase in load. This increase is chosen to simulate a high-stress scenario that tests the resilience of the system.

Five different scenarios are taken into consideration. In Scenario 1, the power system is normally operating without the installation of FACTS devices. In Scenario 2, load shedding has been implemented without the installation of FACTS devices. In Scenario 3, two UPFCs have been installed. In Scenario 4, two SVCs have been installed. In Scenario 5, a combination of SVC and UPFC devices have been installed.

In The first case, the network is maintained without additional devices, and the voltage profile is depicted in Fig. 7 after an increase in the load. It is evident

that Bus 8 had the least voltage, with a value of 0.9 p.u., violating its limits and therefore necessitating corrective control. In 2th to 5th scenario, a suitable location and optimal size of each load that must be shed and FACTS device is obtained by the EOA algorithm introduced previously.

It is pertinent to observe that the rectification of voltage in the bus with the least voltage will lead to deviation from the established limits for voltage correction in other buses. Consequently, in accordance with the flowchart of the proposed methodology, sensitivity analysis is exclusively conducted for Bus 8. The outcomes of this examination are outlined in Table 1 for 10 buses with considerable participation factors values.

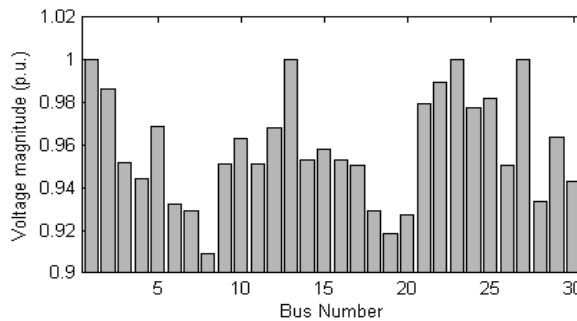


Figure 7. The profile of system voltage after an increase in the load.

Table 1. Sensitivity analysis results

Bus number	Participation factor	Bus number	Participation factor
8	0.1898	19	0.008
10	0.1491	13	0.0072
6	0.1352	28	0.007
4	0.0262	18	0.0065
2	0.0241	12	0.006

In the second scenario, corrective control is implemented through the utilization of a load-shedding algorithm in order to compare and calculate cost savings. The number of buses that had their loads shed, as well as the value of loads to be shed in those buses, is demonstrated in the accompanying table 3. Additionally, the associated cost of load-shedding (calculated at 1000\$ per 100 MW [28]) is also indicated in the table 2.

Table 2. Simulation result of scenario 2.

Bus Number	Values of shed loads		Load Shedding Cost(\$)
	Active power (MW)	Reactive power (MVAR)	
8	51	51	51
19	29.75	5.78	29.75

Bus Number	Values of shed loads		Load Shedding Cost(\$)
	Active power (MW)	Reactive power (MVAR)	
28	4.08	1.53	4.08
TOTAL	848.3	58.31	84.83

In the third and fourth scenarios, the optimal location of a single FACTS device, obtained by employing the EOA algorithm, is considered. In the fifth scenario, two types of FACTS devices are utilized and placed in optimal locations to bolster power system security. The table 3 displays the optimal locations obtained for these scenarios through the utilization of the EOA algorithm.

Table 3. Optimal location of FACTS devices

Scenario	UPFC		SVC	
	# 1	# 2	# 1	# 2
Scenario 3	18 - 19	6 - 28	---	---
Scenario 4	---	---	18	28
Scenario 5	8 - 28	---	7	---

Table 4 illustrates the efficacy of the proposed approach by displaying a comparison of minimum system voltages across different scenarios. Additionally, it displays the annual corrective control cost (F_{it}) and annual saving cost (F_{Saving}) for all scenarios.

Table 4. Optimal location of FACTS devices

Scenario	Minimum Voltage of System		$F_{it}(\$)$	$F_{Saving}(\$)$
	Magnitude (p.u.)	Bus Number		
Scenario 1	8	0.9091	---	---
Scenario 2	30	0.9503	848.3	0
Scenario 3	30	0.9457	336.1	512.2
Scenario 4	30	0.9431	225.9	622.4
Scenario 5	19	0.95	305.2	543.1

This study demonstrates that the employment of FACTS devices for corrective control leads to greater cost savings than optimal load shedding. Furthermore, the results indicate that the installation of one type of FACTS device is insufficient to both improve power system security and maximize annual saving costs. Therefore, it is advisable to install multiple types of FACTS devices at optimal locations in order to enhance system security and maximize annual saving costs.

Conclusion

This research paper presents a comprehensive exploration of a novel strategy for the optimal placement of FACTS devices, which are crucial in enhancing the efficiency and reliability of electrical power systems. The proposed method utilizes the EOA, a sophisticated computational technique that seeks to minimize

costs associated with the integration and operation of these devices. To rigorously evaluate the performance and efficacy of this innovative algorithm, extensive simulations are carried out on the IEEE 30 bus test system, a well-established benchmark in power system analysis. Various scenarios are considered to comprehensively assess how different configurations of FACTS devices could be implemented. The results obtained from these simulations demonstrate a significant potential for the effective deployment of multi-type FACTS devices in improving overall system stability. Furthermore, the findings indicate that this strategic placement not only enhances the operational stability of the power system but also leads to a notable reduction in total costs associated with electricity transmission and distribution. This research contributes valuable insights into the optimization of power systems, emphasizing the balance between technological advancement and economic efficiency. The Future work could explore the integration of FACTS devices with renewable energy sources, dynamic and transient stability analysis, real-time implementation, and comprehensive economic and social impact analysis to further enhance power system resilience and efficiency.

Disclosure statement and funding

The author declares no potential conflicts of interest. The present study received no financial support from any organization or institution.

References

- [1] Amarendra, A., Srinivas, L. R., & Rao, R. S. (2022). *Power system security enhancement in FACTS devices based on Yin–Yang pair optimization algorithm*. *Soft Computing-A Fusion of Foundations, Methodologies & Applications*, 26(13). <https://doi.org/10.1007/s00500-022-07002-1>
- [2] Amarendra, A., Srinivas, L. R., & Rao, R. S. (2022). *Contingency analysis in power system-using UPFC and DVR devices with RDOA*. *Technology and Economics of Smart Grids and Sustainable Energy*, 7(1), 17. <https://doi.org/10.1007/s40866-022-00129-y>
- [3] Afkar, H., & Esmaeeli, M. (2024). *A New Control Strategy for Multifunctional PV Grid Interface Converter Considering Inverter Rating*. *Karafan Journal*, 21(1), 269-296. <https://doi.org/10.1016/j.ijepes.2021.107573>
- [4] Sabzevari, K. (2023). *Improving Reactive Power Sharing in Islanded Microgrid with Transient Reactive Current Injection*. *Karafan Journal*, 20(3), 393-417. <https://doi.org/10.48301/kssa.2023.395017.2536>
- [5] Zhou, Y., Rehtanz, C., Luo, P., Liu, J., Chen, H., Lin, G., Li, Y., & Asmah, M. W. (2022). *Joint corrective optimization based on VSC-HVDC and distributed energy storage for power system security enhancement*. *International Journal of Electrical Power & Energy Systems*, 135, 107573. <https://doi.org/10.48301/kssa.2024.408790.2637>

- [6] Li, X., & Hedman, K. (2020). Enhanced Energy Management System with Corrective Transmission Switching Strategy. 2020 IEEE Power & Energy Society General Meeting (PESGM), <https://doi.org/10.1109/PESGM41954.2020.9281947>
- [7] Ahmadipour, M., Othman, M. M., Salam, Z., Alrifaey, M., Ridha, H. M., & Veerasamy, V. (2023). *Optimal load shedding scheme using grasshopper optimization algorithm for islanded power system with distributed energy resources*. Ain Shams Engineering Journal, 14(1), 101835. <https://doi.org/10.1016/j.asej.2022.101835>
- [8] Pourghasem, P., Seyedi, H., & Zare, K. (2022). *A new optimal under-voltage load shedding scheme for voltage collapse prevention in a multi-microgrid system*. Electric Power Systems Research, 203, 107629. <https://doi.org/10.1016/j.epsr.2021.107629>
- [9] Eid, A., Kamel, S., & Abualigah, L. (2021). *Marine predators algorithm for optimal allocation of active and reactive power resources in distribution networks*. Neural Computing and Applications, 33(21), 14327-14355. <https://doi.org/10.1007/s00521-021-06078-4>
- [10] Hemmati, R., Faraji, H., & Beigvand, N. Y. (2022). *Multi objective control scheme on DFIG wind turbine integrated with energy storage system and FACTS devices: Steady-state and transient operation improvement*. International Journal of Electrical Power & Energy Systems, 135, 107519. <https://doi.org/10.1016/j.ijepes.2021.107519>
- [11] Mutege, M. A., & Nnamdi, N. I. (2022). *Optimal placement of FACTS devices using filter feeding allogenic engineering algorithm*. Technology and Economics of Smart Grids and Sustainable Energy, 7(1), 2. <https://doi.org/10.1007/s00202-020-01072-w>
- [12] Sayed, F., Kamel, S., Taher, M. A., & Jurado, F. (2021). *Enhancing power system loadability and optimal load shedding based on TCSC allocation using improved moth flame optimization algorithm*. Electrical Engineering, 103(1), 205-225. <https://doi.org/10.1007/s40866-022-00132-3>
- [13] Gandotra, R., & Pal, K. (2022). *FACTS Technology: A Comprehensive Review on FACTS Optimal Placement and Application in Power System*. Iranian Journal of Electrical & Electronic Engineering, 18(3). <https://doi.org/10.3390/su14137707>
- [14] Okampo, E. J., Nwulu, N., & Bokoro, P. N. (2022). *Optimal placement and operation of FACTS technologies in a cyber-physical power system: Critical review and future outlook*. Sustainability, 14(13), 7707. <https://doi.org/10.22068/IJEEE.18.3.2390>
- [15] Badrudeen, T. U., Ariyo, F. K., & Nwulu, N. (2024). *Voltage stability improvement and power losses reduction through multiple grid contingency supports*. Energy Exploration & Exploitation, 42(4), 1218-1240. <https://doi.org/10.1504/IJAIP.2024.138572>
- [16] Panthagani, P., & Rao, R. S. (2024). *Optimal allocation of multiple FACTS devices considering power generation pricing for optimal reactive power dispatch using kinetic gas molecule optimisation*. International Journal of Advanced Intelligence Paradigms, 27(3-4), 347-363. <https://doi.org/10.1177/01445987231218292>

- [17] Faramarzi, A., Heidarinejad, M., Stephens, B., & Mirjalili, S. (2020). *Equilibrium optimizer: A novel optimization algorithm*. Knowledge-based systems, 191, 105190. <https://doi.org/10.1016/j.knosys.2019.105190>
- [18] Sen, K. K., & Sen, M. L. (2009). *Introduction to FACTS controllers: theory, modeling, and applications*. John Wiley & Sons. <https://doi.org/10.1002/9780470524756>
- [19] Relić, F., Glavaš, H., Petrović, I., & Stojkov, M. (2025). *Historical Development and Recent Advances in FACTS Technology for Transient Stability in Power Systems*. Tehnički vjesnik, 32(1), 370-380. <https://doi.org/10.17559/TV-20240502001515>
- [20] Javadian, A., Zadehbagheri, M., Kiani, M. J., Nejatian, S., & Sutikno, T. (2021). *Modeling of static var compensator-high voltage direct current to provide power and improve voltage profile*. International Journal of Power Electronics and Drive Systems (IJPEDS), 12(3), 1659-1672. <https://doi.org/10.11591/ijpeds.v12.i3.pp1659-1672>
- [21] Ambriz-Perez, H., Acha, E., & Fuerte-Esquivel, C. R. (2002). *Advanced SVC models for Newton-Raphson load flow and Newton optimal power flow studies*. IEEE transactions on power systems, 15(1), 129-136. <https://doi.org/10.1109/59.852111>
- [22] Nabavi-Niaki, A., & Irvani, M. R. (2002). *Steady-state and dynamic models of unified power flow controller (UPFC) for power system studies*. IEEE transactions on power systems, 11(4), 1937-1943. <https://doi.org/10.1109/59.544667>
- [23] Kamel, S., Jurado, F., Chen, Z., Abdel-Akher, M., & Ebeed, M. (2016). *Developed generalised unified power flow controller model in the Newton-Raphson power-flow analysis using combined mismatches method*. IET Generation, Transmission & Distribution, 10(9), 2177-2184. <https://doi.org/10.1049/iet-gtd.2015.1247>
- [24] Ratnaweera, A., Halgamuge, S. K., & Watson, H. C. (2004). *Self-organizing hierarchical particle swarm optimizer with time-varying acceleration coefficients*. IEEE Transactions on evolutionary computation, 8(3), 240-255. <https://doi.org/10.1109/TEVC.2004.826071>
- [25] Habur, K. (2002). *FACTS for cost effective and reliable transmission of electrical energy*. www.worldbank.org/html/fpd/em/transmission/facts_siemens.pdf. <https://doi.org/10025775070>
- [26] Ali, M. H., Soliman, A. M. A., & Adel, A. H. (2022). *Optimization of reactive power dispatch considering DG units uncertainty by dandelion optimizer algorithm*. International Journal of Renewable Energy Research (IJRER), 12(4), 1805-1818. <https://doi.org/10.20508/ijrer.v12i4.13573.g8606>
- [27] Yorino, N., El-Araby, E., Sasaki, H., & Harada, S. (2003). *A new formulation for FACTS allocation for security enhancement against voltage collapse*. IEEE transactions on power systems, 18(1), 3-10. <https://doi.org/10.1109/TPWRS.2002.804921>
- [28] El-Araby, E.-s. E.-s., Yorino, N., & Sasaki, H. (2003). *A two level hybrid GA/SLP for FACTS allocation problem considering voltage security*. International Journal of Electrical Power & Energy Systems, 25(4), 327-335. [https://doi.org/10.1016/S0142-0615\(02\)00009-1](https://doi.org/10.1016/S0142-0615(02)00009-1)